High-Throughput Epigenetic Profiling Immunoassays for Accelerated Disease Research and Clinical Development

Priscilla Van den Ackerveken[1*], Clotilde Hannart[1], Dorian Pamart[1], Robin Varsebroucq[1], Marion Wargnies[1], Olivia Thiry[1], Marie Lurkin[1], Séverine Vincent[1], Muriel Chapelier[1], Guillaume Rommelaere[1], Marielle Herzog[1].

[1] Belgian Volition SRL, 22 Rue Phocas Lejeune, Parc Scientifique Crealys, 5032 Isnes, Belgium

* Corresponding author email: P.vandenackerveken@volitionrx.com

Running title: New quantitative immunoassays for Histone PTMs.

Abstract:

Epigenetics which examines the regulation of genes without modification of the DNA sequence, plays a crucial role in various biological processes and disease mechanisms. Among the different forms of epigenetic modifications, histone post-translational modifications (PTMs) are important for modulating chromatin structure and gene expression. Aberrant levels of histone PTMs are implicated in a wide range of diseases, including cancer, making them promising targets for biomarker discovery and therapeutic intervention. In this context, blood, tissues, or cells serve as valuable resources for epigenetic research and analysis.

Traditional methods such as mass spectrometry and western blotting are widely used to study histone PTMs, providing qualitative and (semi)quantitative information. However, these techniques often face limitations that could include throughput and scalability, particularly when applied to clinical samples. To overcome these challenges, we developed and validated 13 Nu.Q® immunoassays to detect and quantify specific histone PTM-nucleosomes from K2EDTA plasma samples. Then, we tested these assays on other types of samples, including chromatin extracts from frozen tissues, as well as cell lines and white blood cells

Our findings demonstrate that the Nu.Q® assays offer high specificity, sensitivity, precision and linearity, making them effective tools for epigenetic profiling. A comparative analysis of HeLa cells using mass spectrometry, Western blot, and Nu.Q® immunoassays revealed a consistent histone PTMs signature, further validating the effectiveness of these assays. Additionally, we successfully applied Nu.Q® assays across various biological samples, including human tissues from different organs and

specific white blood cell subtypes, highlighting their versatility and applicability in diverse biological contexts.

Keys words :
Epigenetics, immunoassays, post-translational modifications, histone acetylation, histone methylation, chromatin, biomarker discovery, therapeutic targets, high-throughput epigenetic profiling, nucleosome.

Introduction:

Within the nucleus of eukaryotic cells, genomic DNA is intricately organized into a highly condensed structure known as chromatin. The fundamental unit of chromatin is the nucleosome, which consists of an octamer of core histone proteins (H2A, H2B, H3, and H4) around which approximately 147 base pairs of DNA are tightly wound (1–3). These nucleosomes are connected by stretches of linker DNA and are often stabilized by linker histones such as H1, which further contribute to chromatin's hierarchical structure (4, 5). Given that all cells within an organism have identical DNA sequence, epigenetic regulation is essential for providing each cell its unique identity and specialized function, known as cell-type-specific epigenetic signatures (6, 7). Among the various mechanisms of epigenetic regulation, nucleosome positioning, histone variants and histone post-translational modifications (PTMs) play a central role by modulating chromatin structure (8–11) and are vital for defining and preserving cell identity (7, 12). Disruptions in these mechanisms can lead to disturbances in chromatin organization and gene expression, contributing to pathological conditions and disease development (13–16). Notably, cancer is characterized by these epigenetic changes, which are considered as a hallmark of this disease (17–22). As a result, the altered epigenome of tumor cells is increasingly recognized as potentially effective biomarkers for detecting cancer conditions and classifying tumor types (23–26). Moreover, since such disruptions may be reversible and can be modulated with epigenetic drug treatments (27–31), monitoring epigenetic marks has emerged as a promising target for evaluating cancer therapies, as well as to establish personalized medicine (32–35). Despite significant advances in understanding the key molecular pathways involved in cancer, further research is still necessary to enhance our understanding of the epigenetic signature of tumor cells and to bridge the gap from preclinical models to clinical applications. In this context, patient-derived tissues obtained from surgery or

tumor biopsies provide a valuable and renewable source of material for preclinical analyses, offering an opportunity to directly study tumor-specific epigenetic changes and their clinical relevance. Additionally, isolated peripheral blood mononuclear cells (PBMCs) can inform insights into the underlying mechanisms of the immune response, establishing a complementary model for preclinical research in both cancer (36–38) or other diseases (39, 40).

Several advanced tools are available to characterize epigenetic marks. Chromatin immunoprecipitation (ChIP), combined with either sequencing (ChIP-Seq) or PCR (ChIP-PCR), are invaluable for mapping histone modifications at specific genomic loci, using antibodies to pull down DNA sequences associated with particular histone PTMs and unraveling the intricate relationships between histone modifications and gene regulation (41, 42). Mass spectrometry (MS) provides a complementary approach by enabling the comprehensive analysis of PTMs across the proteome, offering detailed insights into the presence and abundance of these modifications in various cellular contexts (43, 44). However, these methods have limitations, particularly when applied to clinical samples. The low abundance of certain PTMs, along with the complexity of peptide mixtures, often necessitates further validation using additional techniques like Western blot (WB) and immunohistochemistry (IHC). While WB and IHC are useful for detecting and visualizing specific histone PTMs, their low throughput limits their utility in large-scale studies and clinical practice. Given these challenges, immunoassays have emerged as a promising alternative for the study of histone PTMs. These assays offer the opportunity of a reliable and quantitative measure of circulating nucleosomes and their associated epigenetic modifications, combining ease of use with the capacity for high-throughput analysis. Immunoassays could thus facilitate comprehensive profiling of histone PTM patterns and are particularly well-suited for clinical applications, especially for tracking epigenetic patterns in blood (45–48).

In this study, we conducted a comparative analysis of chromatin extracts from HeLa cells using MS, WB, and the Nu.Q® immunoassays. Our findings revealed a consistent histone PTMs signature across all three techniques, underscoring the robustness of these Nu.Q® assays. We then analytically validated 13 Nu.Q® tests for the detection of specific histone PTM-nucleosomes (i.e. 12 Histone-PTMs and 1 Histone-mutation) in K2EDTA plasma samples, demonstrating their performance in terms of specificity, sensitivity, precision and linearity. Additionally, we extended our analysis to chromatin extracts from frozen human tissues of various organ origins, successfully showcasing

the versatility of the Nu.Q® assays in different biological contexts. These assays were further applied to specific white blood cell subtypes, highlighting their effectiveness in diverse epigenetic landscapes. Overall, our study demonstrates that the analytically validated Nu.Q® assays represent a significant advancement in high-throughput epigenetic profiling. These tools have the potential to accelerate disease research and clinical development, offering a transformative asset in the field of epigenetics. Altogether, by analyzing tissue and white blood cells, researchers can leverage these epigenetic tools to gain profound insights into cancer development and identify key therapeutic targets, with the ultimate goal of advancing the field of personalized medicine.

Results:

Nu.Q® Histone PTMs assays, Mass Spectrometry and Western Blotting show consistent outcomes in cell line studies.

The profile of histone PTMs present on the N-terminal tails of Histone H3 in HeLa cell chromatin extracts was first characterized using MS. Through this approach, 29 different histone proteoforms were identified allowing the characterization of 17 distinct histone PTMs located at nine different sites as well as two histone H3 variants (H3.1/H3.2 and H3.3). MS analysis revealed that unmodified and methylated histone H3 peptides were more abundant, whereas acetylated histone H3 peptides were present at much lower levels in these extracts (Figure 1A and Supplementary Figure 1). To further explore the histone H3 PTMs pattern in these cell-derived chromatin extracts, we performed Western blot analysis, which corroborated the MS findings. The WB results demonstrated strong signal intensities for methylated marks on H3 (H3K4Me1, H3K9Me1, H3K9Me3, H3K27Me3, H3K36Me3) and weaker signals for acetylation marks (H3K9Ac, H3K18Ac, H3K27Ac) and citrullination marks (H3R8Cit) (Figure 1B and Supplementary Figure 1). We then quantified the histone PTMs-nucleosome pattern using Nu.Q® immunoassays, which further confirmed the epigenetic profile observed by MS and WB (Figure 1C). Indeed, the Nu.Q® assays results revealed low levels of acetylated histone H3 nucleosomes (n=4; mean±SD : H3K9Ac= 0.81±0.10%, H3K18Ac= 0.52±0.10%, H3K27Ac= 0.21±0.04%) and H3R8Cit-nucleosomes (n=4; mean±SD: H3R8Cit= 1.84±0.43%). In contrast, higher

proportions of methylated histone H3 nucleosomes were observed (n=4; m<ean±SD: H3K4Me1= 10.46±1.42%; H3K4Me2= 3.34±0.56%; H3K9Me1= 21.49±3.62%; H3K9Me3= 40.88±4.07%; H3K27Me3= 31.04±2.16% and H3K36Me3= 25.39±1.87%). The comparison of the three analytical techniques - MS, WB and Nu.Q® immunoassays analyzed as the ratio of the histone PTMs to the total H3 peptides/protein/H3.1-nucleosome, reveals a consistent nucleosome pattern across all three methods (Figure 1D). Given the low endogenous expression of acetylated histone H3 in HeLa cells, we aimed to determine whether the consistency of the results observed with methylated histone H3 could be extended to acetyl-markers under conditions of induced acetylation. For that purpose, HeLa cells were treated with sodium butyrate (NaB), a histone deacetylase (HDAC) inhibitor, and the levels of three acetylated nucleosomes and two methylated nucleosomes were quantified using Nu.Q® immunoassays. As expected, NaB treatment led to a significant upregulation of all tested acetylated H3 nucleosomes ratio (n=3; mean±SD untreated vs NaB-treated : H3K9Ac= 0.88±0.69% vs 85.08±18.20% (****: $p < 0.0001$); H3K18Ac= 1.35±1.42% vs 109.22±10.85% (****: $p < 0.0001$); H3K27Ac= 0.33±0.54% vs 22.11±8.02% (*: $p < 0.05$)) while methylated H3 nucleosome ratio levels remained relatively constant (n=3: mean±SD untreated vs NaB-treated: H3K27Me3= 18.86±11.94% vs 31.08±5.86% (ns: p=0.1585); H3K9Me3= 25.88±17.37% vs 35.38±7.06% (ns: $p = 0.2685$)) (Figure2A). The results obtained by WB and their associated quantification, normalized to total H3 protein levels, reflect these findings (Figure 2B and Supplementary Figure 2). Altogether, the results demonstrate the capability of Nu.Q® immunoassays to accurately characterize histone PTMs in cell lines, delivering results consistent with those obtained through MS and WB.

Nu.Q® Histone PTMs assays are analytically validated chemiluminescent immunoassays that allow a specific, precise quantification of histone-PTMs in plasma samples.

The analytical performance of 13 different chemiluminescent immunoassays (ChLIA) tests (Nu.Q®) was rigorously evaluated in K2EDTA plasma samples. First, we assessed the specificity of each assay using recombinant nucleosomes (rNucl.) that exhibit specific histone PTMs, histone variants, or the H3K27M mutation. The Nu.Q® assays demonstrate minimal/no cross-reactivity, with most assays showing no or

negligible cross-reactivity (ranging from 0% to 3%) (Figure 3A). An exception is the Nu.Q® H3K27Ac assay, which exhibits a slight cross-reactivity with the rNucl. H3K27M (8% cross-reactivity). Additionally, the results confirm that the Nu.Q® H3.1 assay recognizes all recombinant PTMs-H3.1 nucleosomes, except the H3.3 variant, with 0% cross-reactivity observed. The precision of the 13 different Nu.Q®PTMs assays was then assessed by determining the within-run (Intra-CV) and within-laboratory (Inter-CV) coefficients of variation. The Intra-CV values range from 0.9% to 7.6%, while the Inter-CV values vary from 1.4% to 16.1% (Figure 3B), indicating high consistency and reliability of the assays. Then, the sensitivity of the 13 assays was evaluated, demonstrating good detection performance with a LOB ranging from 0.10 to 1.90 ng/mL; a LOD from 0.80 to 3.57ng/mL and a LOQ from 0.8 to 8.1 ng/mL defined as the assay limit (Figure 3C). Additionally, we determined the linear range of each Nu.Q®PTMs assay using K2EDTA plasma samples (Figure 3D), and the linearity of the assay curves was confirmed, with R^2 values ranging from 0.9985–1.00 across all assays. Overall, these analytical performances confirm that the 13 Nu.Q®PTMs ChLIA assays are highly precise and specific for the measurement of histone PTMs and histone mutation-nucleosome concentrations in plasma samples.

Effective histone PTMs analysis using Nu.Q®PTMs assays on chromatin extracted from human fresh-frozen tissues.

To validate the applicability of Nu.Q®PTMs assays beyond plasma and cellular extracts, we examined nucleosome modification patterns in fresh-frozen human tissues from various organs. First, we confirmed that our optimized chromatin extraction protocol produces consistent mononucleosome extracts (~150bp) across different tissue types, as demonstrated by the comparable DNA profiles obtained using a bioanalyzer (Figure 4A and Supplementary Figure 3). Subsequent characterization of histone PTMs/mutations marks revealed a range of modification levels across the tissues. High to moderate levels were observed for H3K27Me3- (range from 11.33% to 95.13%) and H3K36Me3-nucleosomes (range from 13.37% to 173.90%). Moderate to low levels were found for H3R8Cit- (range from 0.03% to 11.77%), H3K27Ac- (range from 0.12% to 9.31%) and H3K9Me3- nucleosome (range from 0.67% to 17.19%). Low levels were detected for H3K4Me2- (range from 0.98% to 6.03%), H3K9Me1- (range from 0.37% to 5.58%), H3K4Me1- (range from 0.38% to 3.19%), H3K18Ac- (range from 0.2% to 4.45%), H3K9Ac-nucleosomes (range from 0.46% to 2.31%) (Figure 4B).

In addition, the H3K27M, pH2Ax and H3S10ph-nucleosome markers were not detected in any of the tissues (Data not shown). Interestingly, we observed considerable heterogeneity in the epigenetic patterns across different tissue types and patients, with coefficients of variation ranging from 45% for H3K9Ac-nucleosomes to 226% for H3K27Ac-nucleosomes. Together, these findings suggest that the Nu.Q®PTMs assays are effective in characterizing histone PTMs marks across various human tissues.

Histone PTMs insights from subpopulation of white blood cells enabled by cutting-edge Nu.Q®PTMs assays.

To explore the broader utility of our Nu.Q®PTMs assays, we investigated epigenetic patterns in various white blood cell subpopulations. We began by determining the minimal cell count required for efficient chromatin extraction from human peripheral blood mononuclear cells (PBMCs) by testing three different cell quantities (1; 2 and 5 million cells). The DNA profiles obtained from these extractions were analyzed using a bioanalyzer, which consistently confirmed the presence of a mononucleosome peak (~150bp) in all cases (Figure 5A). Following this confirmation, we measured the amount of H3.1-nucleosomes using the Nu.Q® H3.1 assay and observed a proportional increase in nucleosome quantity with higher cell counts (Figure 5B). Next, we profiled the histone PTMs pattern in PBMCs, two monocyte subsets isolated from PBMCs and the non-isolated residual cells (referred to as Monocyte-depleted PBMCs) using the panel of 13 Nu.Q®PTMs assays. Results show that the tested PBMCs exhibit high levels of H3K27Me3- (11.73% of nucleosome) and H3K36Me3-nucleosomes (29.3% of nucleosome). Monocytes display higher levels of several modifications compared to Monocyte-depleted PBMCs, specifically H3R8Cit- (n=2; mean±SD: monocyte vs Monocyte-depleted PBMCs: 3.40%±2.35% vs 0.89%±0.11%); H3K9Me3- (n=2; mean±SD: monocyte vs Monocyte-depleted PBMCs: 20.76%±1.66% vs 2.59%±0.67%); H3K9Me1- (n=2; mean±SD: monocyte vs Monocyte-depleted PBMCs: 15.52%±0.22% vs 2.38%±2.09%) and H3K4Me1- nucleosome (n=2; mean±SD: monocyte vs Monocyte-depleted PBMCs: 4.84%±1.52% vs 0.60%±0.05%). In addition, the Nu.Q® H3K27M, Nu.Q® pH2Ax and Nu.Q® H3S10ph markers were not detected in any of the cell extracts (Data not shown). Together, these data suggest that the Nu.Q®PTMs assays effectively characterize histone PTMs marks across different subpopulations of white blood cells.

Discussion

Epigenetics is a promising field for patient care, offering potential breakthroughs in the diagnosis, identification of novel therapeutic targets and improved treatment monitoring of a wide range of diseases (14, 49, 50). Histone post-translational modifications represent a crucial epigenetic mechanism with strong diagnostic potential (49, 51) as abnormal histone-PTMs patterns are frequently linked to a range of diseases, such as cancer, neurological disorders, and inflammatory conditions (13, 14, 21, 22, 52–56). To study these epigenetic changes, particularly histone-PTMs, several advanced research methods are used such as ChIP-Seq/ChIP-PCR, MS or WB (57–62). In this study, we propose to use sandwich immunoassays to quantify specific histone-PTMs associated with nucleosomes as new powerful tools for epigenetic characterization of circulating nucleosomes, as well as chromatin extraction from cell lines to white blood cells subpopulations and human tissues. Using cell line extracts, we first compared the WB analysis of anti-histone PTMs and MS data to the Nu.Q® immunoassay results, observing a similar epigenetic pattern across all three methods. MS has emerged as a powerful tool for the unbiased and quantitative evaluation of proteins and their PTMs (44, 63, 64). However, this technique involves a complicated process to reduce the sample's protein complexity such as enrichment of nucleosomes (47, 65) or fractionation using SDS-PAGE gel or ultra-HPLC separation (66), which can potentially lead to the loss of sensitive PTMs (67). Additionally, the pretreatment required to handle high lysine content and reduce interfering reagents like high salt or detergents (67–69) combined with the presence of isobaric peptides (57) can complicate the accurate assignment of PTMs and make relative quantification of PTMs more challenging (44). As a result, MS often requires validation by another technique, such as WB or immunoassays to ensure accurate identification and quantification of PTMs. WB is widely used to study histone PTMs, but its lack of high-throughput capability and limited linear range make analyzing multiple PTMs costly, labor-intensive, and less accurate (70–72). In contrast, immunoassays are commonly used to evaluate the levels of circulating biomarkers for diagnosis, prognosis or treatment follow-up (73–75). Following rigorous development and analytical validation, the immunoassay offers several advantages, including high sensitivity, achieved through amplification via a labeling system, high specificity, shorter turnaround times, simpler procedures, and automation that enables to high-throughput capability. These

characteristics make immunoassays highly specific and sensitive, rendering them the methods of choice for measuring complex molecules (76, 77). In this study, we validated 13 specific immunoassays that are highly sensitive in detecting specific histone post-translational modifications associated with circulating nucleosomes. These assays are designed to be simple, low-cost and easily accessible, requiring only a minimal sample volume of 50µl. They offer the advantages of automation and rapid processing, delivering reliable results in less than one hour, making them suitable for routine testing. By applying validated immunoassays across a variety of biological samples, ranging from human tissues to specific white blood cell subtypes, we demonstrated the versatility of these assays in epigenetic profiling. In tumor tissues, we observed a different proportion of acetylation and methylation of the histone H3 across different organs. Consistently with our findings, a low proportion of acetylation has been described as a marker of cancer progression and identified as a potential prognostic factor in many types of solid tumors (50). In parallel, we observed a global high level of H3K27Me3 and H3K36Me3, two antagonistic histone PTMs, which play a significant role in carcinogenesis, with their dysregulation potentially contributing to tumor progression (78–81). Since histone PTMs can have opposite effects depending on the tumor type (50, 82, 83), more in depth clinical studies and tissues-specific characterization are required to identify either potential biomarkers or therapeutic targets. These tools promise to advance disease research and clinical development, providing a groundbreaking resource in epigenetics.

List of abbreviations:

Ac	Acetyl
bp	Base pair
BSA	Bovine serum albumin
ChIP	Chromatin immunoprecipitation
ChLIA	Chemiluminescent immunoassays
Cit	Citrullination
CV	Coefficients of variation
dsDNA	double-stranded DNA
FA-PBS	PBS – Formaldehyde

HDAC	Histone Deacetylase
IHC	Immunohistochemistry
K	Lysine
LC-MS/MS	Liquid chromatography with tandem mass spectrometry
LOB	The Limit of Blank
LOD	The Limit of Detection
LOQ	The Limit of Quantification
Me1/Me2/Me3	Methyl ; 2 Methyl ; 3 Methyl
MNAse	Micrococcal nuclease
MS (/ MS)	(Tandem) Mass spectrometry
NaB	Sodium butyrate
NAT	Normal Adjacent Tissue
ns	Non-significant
PBMCs	Peripheral blood mononuclear cells
PBS	Phosphate-buffered saline
PCR	Polymerase chain reaction
PTMs	Histone post-translational modifications
rNucl.	Recombinant nucleosomes
RT	Room Temperature
SD	Standard Deviation
SDS-PAGE	Sodium dodecyl-sulfate polyacrylamide gel electrophoresis
Seq	Sequencing
TBST	Tris Buffer Saline + 0.1% Tween® 20
ultra-HPLC	Ultra-High-Performance Liquid Chromatography
WB	Western blotting
WBC	White blood cells

Material and method

Samples and cells collection

Frozen human PBMCs, diluted in 60% RPMI-1640, 35% FBS and 5% DMSO, and fresh-frozen human tissues were purchased from Biomedica CRO, a biobank that presents a full compliance with the international and local ethical guidelines (approval by the IRB/IEC). HeLa S3 cells (ATCC, #CCL-2.2) were cultured in S-MEM medium (Gibco, #11380037) supplemented with 10% Fetal Bovine Serum (Gibco, #A4766801), 1x NEAA (Non-Essential Amino Acids solution) (Gibco, #11140-050), Penicillin/Streptomycin (Gibco, #15070063) and 1x L-glutamine (Gibco, #25030081), with or without NaB treatment (5mM as final concentration, for 20h; Merck Life Sciences BV; #19-137). HeLa S3 cells were maintained in a CO_2 incubator (37°C, 5% CO_2).

Monocytes isolation

After evaluating the number of frozen PBMCs cells using the NanoEnTek, EVE TM Plus system, the cells were centrifuged at 200g for 10 minutes, and the cell pellet was resuspended on 1mL of isolation buffer (phosphate-buffered saline (PBS), pH 7.2, 0.5% bovine serum albumin (BSA) (VWR; #4215015), 2mM EDTA (Merck Life Sciences BV; #E7889)) and recentrifuged to pellet PBMCs. Monocytes were then isolated following Pan-Monocyte Isolation Kit instructions (Miltenyi; 130-096-537).

Chromatin extraction

From cells (i.e. PBMCs, monocytes and/or HeLa cells): After cell counting (NanoEnTek; EVE TM Plus), cells were centrifuged for 5 minutes at 150 g and washed with 1mL of cold PBS. For each 2.5 x10^7 cells, cells pellets were resuspended on 300µl of lysis buffer (10mM HEPES pH 7.4, 10mM KCL, 1mM Sodium orthovanadate, 0.05 % Igepal (Merck Life Sciences BV; #i8896), EDTA-free cOmplete^{TM} (Roche; #4693159001)) and incubated for 20 minutes on ice before being centrifuged again at 12,000 g for 10 minutes. This was followed by an additional wash cycle involving a lysis buffer, incubation, and centrifugation steps. Cells pellet was then resuspended on 600µL of low salt buffer (10mM Tris-HCl pH 7.4, 0.2mM MgCl2, 1mM Sodium orthovanadate, 1% Triton (Merck Life Sciences BV; #T8787) + EDTA-free cOmplete^{TM} (Roche; #4693159001)) and incubated on ice for 15 minutes before being centrifuged again at 12,000 g for 10 minutes. Then, the cells pellet was resuspended on 100µL MNAse digestion buffer (5mM CaCl2, 50mM Tris-HCl pH 8, 1mM sodium

orthovanadate + EDTA-free cOmplete™ (Roche; #4693159001)). Finally, 0.155U of MNAse (Merck Life Sciences BV; #N5386) was added to each sample, and incubate at 37°C for 15 min. After that step, 50µL of EDTA 0.5M (Merck Life Sciences BV; #E7889-100ml) were added to the mixture and incubate 5 minutes on ice to stop MNAse reaction. Nucleosomes were then recovered on supernatant after centrifugation at 9,000g for 5 minutes. For NaB treated HeLa S3 treated, 5mM of NaB (Merck Life Sciences BV; #19-137) was added to all extraction buffers (i.e. Lysis buffer, Low salt buffer and MNAse digestion buffer).

From Fresh Frozen tissues: 100mg of frozen tissues were fixed with 40µL of 1% PBS – formaldehyde (FA-PBS) (Merck Life Sciences BV; #F8775) and then finely chopped with little scissors. Then, 900µL of 1% FA-PBS was added to the tissues and the tissues were fixed for 10 minutes at RT on a rotating wheel. Subsequently, 0.125M of Glycine (Cytiva; #GE17-1323-01) was added and incubated for an additional 10 minutes on a rotating wheel. Following this, a wash (500µL of PBS + 1% of protease inhibitor cocktail (Merck Life Sciences BV; #P8340)) and centrifugation cycle (12,000g for 2 min) was performed three times consecutively. After that, the fixed tissues were incubated with either 1mL of 1% collagenase/Dispase-PBS (Roche; 10269638001) containing 0.1% of CaCl2 1M (Merck Life Sciences BV; #C1016-500g) for 30 minutes at 37°C (i.e. Rectum, pancreas and small intestine tissues) or 500µL of trypsin-EDTA (Thermo Fisher Scientific; 25300-054) for 10 min at 37°C (i.e. Kidney, lung, uterus and prostate tissues). Tubes were then centrifuged at 12,000g for 5 minutes and supernatant was discarded. A last wash with PBS-1% protease inhibitor was performed. Tissues pellet was resuspended on 360µL of lysis buffer (10mM HEPES pH 7.4, 10mM KCL, 1mM Sodium orthovanadate, 0.05 % Igepal, EDTA-free cOmplete™) and mechanical disruption was performed using a homogenizer with a pestle adapter (BELART; #651000000) followed by an incubation on ice for 20 min. After a centrifugation at 12,000g for 10 minutes and a wash step with lysis buffer, tissue pellets were then resuspended on 720µL of low salt buffer (10mM Tris-HCl pH 7.4; 0.2mM MgCl2, 1mM Sodium orthovanadate, 1% Triton, EDTA-free cOmplete™). After an incubation of 15 minutes on ice and a centrifugation at 12,000g for 10 minutes, tissues pellets were resuspended on 120µL MNAse digestion buffer, 0.2U of MNAse (Merck Life Sciences BV; #N5386) were added to each sample, and incubate at 37°C for 30 min. After that step, 12µL of EDTA 0.5M (Merck Life Sciences BV; #E7889) were

added to the mixture and incubate 5 minutes on ice to stop MNAse reaction. Nucleosomes were then recovered on supernatant after centrifugation at 9,000g for 5 minutes.

Nucleosomes quantification

H3.1-Nucleosomes level (Nu.Q® H3.1) and specific PTMs-nucleosomes were quantified by Nu.Q® immunoassays (Nu.Q® -H3K27Me3, -H3K36Me3, -H3K4Me2, -H3K9Me3, -H3K9Me1, -H3K4Me1, -H3K18Ac, -H3K9Ac, -H3K27Ac, -H3K27M, -H3R8Cit; -ph2Ax, -H3S10ph) according to the manufacturer's instructions (Belgian Volition SRL, Isnes, Belgium), after dilution of chromatin extract in a plasma-diluent (Seracon II Delipidated, Seracare; #1800-0017).

Analytical performances

Sensitivity limits were established following the recommendations in CLSI guideline EP17-A2 with some modifications. Briefly, to determine the Limit of Blank (LOB), >10 diluent measurements over 5 days were averaged, with the LOB set as the average plus 1.645 standard deviations. The Limit of Detection (LOD) was determined by testing non-blank samples of low concentrations over five days, for a minimum of 30 measurements overall. The pooled standard deviation for all measurements was calculated, and the LOD was determined as LOD = LOB + 1.645 times the pooled SD of non-blank samples. Finally, the lower limit of quantification (LOQ) was defined using a precision profile, with a maximum allowable imprecision of 20% CV for precise quantification.

Precision was evaluated via measurement of 4-6 samples displaying different concentration levels, after spiking on human K2EDTA plasma samples with native nucleosomes isolated from human cells or recombinant nucleosomes. The spiked samples were quantified across a minimum of 5 days, with two runs per day and 3 measurements per run. CV% were determined based on CLSI-EP05A guidelines, using an "Analysis of variance" with the Analyse-it software, to assess within-lot and within-laboratory precision. The table presented in the main Figure 3B shows the min to max %CV obtained for each Nu.Q®PTMs Assay.

To assess linearity, human K2EDTA plasma samples of varying concentrations were blended in equal proportions (at 10% intervals) and linear curve fitting with variance-based weighting were applied. The linear ranges were defined through comparison of measured concentrations of the different sample proportions with linear regression expected concentrations. The linearity range specifies the interval where the deviation between actual measurements and predictions from the linear model is under 10%. Figure 3D shows a visual representation of linear ranges found on each immunoassay for 1 representative sample. The R^2, also called Pearson's linear coefficient of determination, measures the strength of the linear relationship between the response variable (Y) and the predictor variable (X) on the linearity range determined. This value stands between 0 and 1 and therefore makes it possible to evaluate the relevance of the linear model for the dilutions of our samples.

Specificity: The cross-reactivity was assessed by quantifying single recombinant nucleosome (rNucl.; (Belgian Volition SRL, Isnes, Belgium)) exhibiting either a variant modification (H3.1 or H3.3 histone) or PTMs or Mutation (H3K27M) using the Nu.Q® assay panel. All Nu.Q® tests were conducted simultaneously using the same rNucl. , diluted at 1µg/mL in a plasma diluent (Seracon II Delipidated, Seracare; #1800-0017) preparation.

Characterization of Histone post-translational modifications by Liquid chromatography with tandem mass spectrometry (LC–MS/MS)

HeLa cells nucleosomes were extracted following previously described protocol, and were then processed by EpiQMAx GmbH (Planneg, Germany) to analyze the histone post-translational modifications pattern by LC–MS/MS. Nucleosomes were propionylated and trypsinized. Heavy amino acid-labeled peptides were added to digested samples for normalization and quantifications purposes. The resulting mixture was separated by liquid chromatography (Ultimate 3000 RSLC nano System (Thermo-Fisher Scientific) containing a 15-cm analytical column (75 µm ID with ReproSil-Pur C18-AQ 2.4 µm from Dr. Maisch) directly coupled to an electrospray ionization source and Q Exactive HF mass spectrometer (Thermo-Fisher Scientific). A data-dependent acquisition mode was used to automatically switch between full scan MS and MS/MS acquisition. For the analysis, the raw peptides of canonical histone peptides and their respective PTMs intensities were searched with Skyline software and normalized using the intensities of corresponding spiked-in heavy peptides. For peptides without spiked-

in heavy standards (e.g., from H4), normalization was done using the overall intensity trend of the heavy standards. The ratios of light/ heavy peptide were then normalized over their average value across all samples and the log2 values were calculated.

Western Blotting

200ng of chromatin extract were mixed with Laemmli buffer (Biorad; #1610747) containing 10% of 2-mercaptoethanol (Merck Life Sciences BV; #M6250) and denaturated for 5 minutes at 95°C. Denatured nucleosomes were separated by electrophoresis on 4-20% TGX precast gels (Biorad; #4561094) under reducing conditions (Tris/Glycine/SDS; Biorad; #1610772) and then transferred to PVDF (polyvinylidene fluoride) membranes using a Trans-Blot Turbo semi-dry transfer system (Biorad; #1704272). The PVDF membranes was then incubated 2 hours with antibodies against H3K27Me3 (Cell Signaling Technology; #9733BF – lot: 25), H3K36Me3 (Active Motif; #80218 – lot: 2280106), H3K9Me3 (Abcam; #232324 – lot: GR3452452-1), H3K4Me2 (Volition; #3349 lot: rr260604a-6240), H3R8Cit (Abcam; #232939 – lot: GR3402039-3), H3K27Ac (Volition; #3118– lot: rr200819b-6298), H3K18Ac (Synabs; #FYN213R CL3 lot: 10487), H3K9Ac (Active Motif; #91103 – lot: 22420006), H3K9Me1 (Cell Signaling Technology; #14186BF – lot: 5), H3K4Me1 (Cell Signaling Technology; #5326BF – lot: 4), diluted on Tris Buffer Saline, 1% of Casein (Biorad; #1706435) + 0.1% Tween®20 (Merck Life Sciences BV; #T2700) at 2µg/ml and incubated for 2H at RT or overnight at 4°C. After primary antibody incubation, membranes were washed three times with 1x TBST ((Biorad; #1706435) + 0.1% Tween®20 (Merck Life Sciences BV; #T2700)) and incubated with a detection reagent (VeriBlot antibody for IP Detection Reagent, Abcam; #ab131366) or anti-rat HRP antibody (for H3K18AC detection; Jackson immunoresearch, 112-035-003 – lot: 146459) for 1 hour at RT. Membranes were again washed three times with TBST and incubated with Super Signal West Dura Extended Duration Substrate for 5 minutes (Life Technologies Europe, #34076). Chemiluminescent signals were acquired with the Fusion-FX6 instrument and software (Vilber). All membranes were then stripped to remove detection antibodies by incubating twice for 10 minutes with a mild stripping buffer (Glycine 0.2M, SDS 0.1%, Tween®20 1%, pH 2.2), followed by two washes on 1x PBS and 2 washes on 1x TBST. Stripped membranes were then reincubated with anti-H3 C-terminal antibody (Active Motif; #91297 – lot: 316202) diluted at 1.5µg/ml on

TBS, 1% of Casein (Biorad; #1706435) + 0.1% Tween®20 (Merck Life Sciences BV; #T2700). The following steps were the same as previously described for all detection antibodies. To validate the specificity of the detected signals, recombinant nucleosomes specific to each PTMs were loaded on a separate lane (data not shown). Western-blots were quantified using Bio-1D quantification program (Vilber Lourmat) and normalized based on associate H3C-terminal band signal.

Nucleosomal DNA extraction and DNA size profile

Chromatin extracts were diluted on 1x PBS and extracted with QIAamp® DSP Circulating NA kit (Qiagen; #61504) following manufacturer's instructions. The subsequent DNA size distribution was analyzed by using Agilent High Sensitivity DNA Kit for fragment sizes of 50 - 7000bp (Agilent Technologies; #5067-4626) with the Agilent 2100 Bioanalyzer (Agilent Technologies), following the manufacturer's instructions.

Statistical analysis :

Heat map analysis were performed using GraphPad InStat software (GraphPad Software, USA). Mass spectrometry data are represented as Log2 of intensity. Nu.Q® PTMs are represented as a ratio (%) of Nu.Q® PTMs/Nu.Q® H3.1. Specificity data are represented as the % of cross-reactivity. The cross-reactivity was measured and calculated by dividing the concentration of rNucl. exhibiting unspecific PTMs by the concentration obtained for rNucl. exhibiting specific PTMs (%).

The MS barplot shows the % of the relative PTMs quantitation defined as ratios of the summation of PTMs ions abundances over the total intensity of all peptides of identical sequence. The WB *barplot* shows the % of the relative PTMs quantitation defined as ratios of the PTMs over the H3-C-terminal signal. Nu.Q® PTMs barplot are represented as a ratio (%) of Nu.Q® PTMs/Nu.Q® H3.1.

Multiple unpaired t-tests, using GraphPad InStat software (GraphPad Software, USA), were conducted to evaluate the effect of NaB on the epigenetic profile in HeLa cells (*$p < 0.05$; **$p < 0.01$; ***$p < 0.001$).

Acknowledgments

We would like to thank Virginie Laloux and Fanny Lambert for their work in cultivating and amplifying HeLa cells. We thank the Administrative and Logistics team of Belgian Volition for their support. We thank Moritz Völker-Albert and the EpiQMAx's team for MS data acquisition and their assistance in drafting the MS material section. We thank Louise Batchelor for her careful proofreading of the manuscript. OpenAI *ChatGPT* GPT-4 was used to support minor edits throughout the manuscript.

CRediT Author statement

Conceptualization : P.VdA; Analysis and interpretation of data: D.P., C.H., G.R., M.W. and P.VdA.; resources and data acquisition: C.H., M.L. ,O.T. ,R.V. , S.V. and M.C. ; writing original draft: P.VdA, M.W., C.H. and D.P., writing-review and editing D.P. ; C.H., G.R., R.V., M.W., O.T. M.L., S.V., M.C., M.H. and P.VdA. Supervision: M.H. All authors have read and approved the manuscript.

Additional information: declaration of Interests
All authors are employed by Belgian Volition SRL. Belgian Volition SRL has patents covering Nu.Q® technology and are developers of Nu.Q® assays. Belgian Volition SRL is a subsidiary of VolitionRx Limited. MC and MH are shareholders of VolitionRX Limited.

Data availability:

The datasets used and/or analyzed during the current study are available from the corresponding author on reasonable request.

Figures legends:

Figure 1. Histone-PTMs profile present in the N-terminal tails of histone H3 from HeLa cells chromatin extracts as defined by Mass Spectrometry (LC-MS/MS), Western Blotting (WB), and Nu.Q® Histone-PTMs assays.

A. The heat map illustrates the relative intensity of histone PTMs detected by LC-MS/MS. Raw intensities are represented on a log2 scale, with each cell corresponding to a specific histone PTM across four different HeLa cell chromatin extracts (HeLa #1-4). Gray cells indicate undetected histone-PTMs.

B. Western blot analysis targeting 10 different PTMs of the histone H3 N-terminal tail. Each column represents a different HeLa cell chromatin extract preparation (HeLa #1-4) with a representative result for Histone H3 (H3). Control blots targeting the C-terminal end of histone H3 (H3) were included in all WB experiments to ensure

equivalent loading between the conditions. Each line represents a cropped gel/blot picture (upper/lower marker: 20kDa-15kDa) of. The quantitative analysis of the Western blot results is shown alongside in Supplementary Figure 1.

C. Quantification of histone PTMs using specific Nu.Q® immunoassays. Each lane represents a different HeLa cell chromatin extract preparation (HeLa #1-4). The heat map illustrates the relative quantification of each PTM normalized to the H3.1 quantification (%).

D. A histogram compares histone PTMs levels across the three detection techniques: MS (black bar, ratio (%) of the PTMs intensity per peptide), WB (gray bar; ratio (%) of histone PTMs to H3-C terminal), and immunoassays (red bar; ratio (%) of assay-specific PTMs to the Nu.Q® H3.1 level). Each bar represents the average PTM level across the three techniques, with error bars indicating standard deviation (SD) (n= 4 cellular extracts).

Figure 2. Evaluation of Histone H3 PTMs in HeLa cells treated with Sodium Butyrate (NaB).

A. Quantification of Histone H3 Acetylation (H3K27Ac, H3K9Ac, H3K18Ac) and Methylation Levels (H3K9Me3, H3K27Me3) using Nu.Q® Immunoassays (ratio (%) of assay-specific PTMs to the Nu.Q® H3.1 level) in HeLa cells treated with NaB (Red) vs untreated cells (Gray). Each bar represents the average PTM levels across the three replicates, with error bars indicating standard deviation (SD)(n= 3, Multiple unpaired t-test; $^{**}p < 0.01$; $^{***}p < 0.001$; ns: not significant).

B. Western Blot analysis of Histone H3 Acetyl and Methyl PTMs with a representative result for Histone H3 (H3). The C-terminal end of histone H3 (H3) were included in all WB used as loading control. Each line represents a cropped gel/blot picture (upper/lower marker: 20kDa-15kDa) ofWB . Each column represents a different HeLa cell chromatin extract preparation from cells untreated (first #1-#3) or treated with NaB (last #1-#3lanes, +NaB). The quantitative analysis of the Western blot results is shown alongside in Supplementary Figure 2.

Figure 3. Analytical validation of Nu.Q® Histone PTMs Chemiluminescent Immunoassays (ChLIA).

A. The heat map illustrates the specificity of Nu.Q®H3.1 and 13 Nu.Q®PTMs chemiluminescent immunoassays tested against recombinant nucleosomes (rNucl.) with various histone post-translational modifications, histone variants, and the H3K27M mutation. Results show the % of cross-reactivity among the Nu.Q® assays.

B. Min. and Max. of the Intra-assay (Intra-CV) and inter-assay (Inter-CV) coefficients of variation for each of the 13 Nu.Q®PTMs assays.

C. Limits of blank (LOB), limits of detection (LOB) and limits of quantification (LOQ) estimated for all Nu.Q®PTMs assays.

D. Linearity range of the assays and the related R^2 values for all curves.

Figure 4. Nucleosome modification patterns in fresh-frozen human tissues from several organ origins.

A. dsDNA Fragment size distribution of representative chromatin extract from several tissue origine using Agilent 2100 Bioanalyzer. Additional electropherograms are shown in Supplementary Figure 3.

B. The heat map illustrates the relative quantification (%) of each PTM normalized to the H3.1 quantification (lines) in chromatin extracts from different human tissue types (column) including Tumor tissues and Normal adjacent tissues (NAT).

Figure 5. Histone PTMs profiling in white blood cell subpopulations using Nu.Q® assays.

A. dsDNA Fragment size distribution of dsDNA chromatin extract from multiple number (i.e. $1x10^6$, $2x10^6$, $5x10^6$) of extracted PBMCs cells using Agilent 2100 Bioanalyzer.

B. Histogram showing the proportional increase in H3.1-nucleosome levels as measured by the Nu.Q® H3.1 assay across increasing PBMC counts (from $1x10^6$ to $5x10^6$ cells).

C. Heat map illustrating the relative quantification (%), of each histone PTMs normalized to the H3.1 quantification, from PBMCs, two isolated monocyte subsets, and the remaining non-isolated white blood cells (referred to as Monocyte-depleted PBMCs).

Supporting Information : This article contains supporting information.

References:

1. Wolffe, A. P., and Hayes, J. J. (1999) Chromatin disruption and modification. *Nucleic Acids Res*. **27**, 711–720
2. Bradbury, E. M. (1989) K. E. Van Holde. Chromatin. Series in molecular biology. Springer-Verlag, New York. 1988. 530 pp. $98.00. *Journal of Molecular Recognition*. 10.1002/jmr.300020308
3. Luger, K., Mäder, A. W., Richmond, R. K., Sargent, D. F., and Richmond, T. J. (1997) Crystal structure of the nucleosome core particle at 2.8 Å resolution. *Nature*. **389**, 251–260
4. Thoma, F., Koller, T., and Klug, A. (1979) Involvement of histone H1 in the organization of the nucleosome and of the salt-dependent superstructures of chromatin. *J Cell Biol*. **83**, 403–427
5. Quina, A. S., Buschbeck, M., and Di Croce, L. (2006) Chromatin structure and epigenetics. *Biochem Pharmacol*. **72**, 1563–1569
6. Spivakov, M., and Fisher, A. G. (2007) Epigenetic signatures of stem-cell identity. *Nat Rev Genet*. **8**, 263–271
7. Margueron, R., Trojer, P., and Reinberg, D. (2005) The key to development: interpreting the histone code? *Curr Opin Genet Dev*. **15**, 163–176
8. Hebbes, T. R., Thorne, A. W., and Crane-Robinson, C. (1988) A direct link between core histone acetylation and transcriptionally active chromatin. *EMBO J*. **7**, 1395–1402
9. Strahl, B. D., and Allis, C. D. (2000) The language of covalent histone modifications. *Nature*. **403**, 41–45
10. Grunstein, M. (1997) Histone acetylation in chromatin structure and transcription. *Nature*. **389**, 349–352
11. Bai, L., and Morozov, A. V. (2010) Gene regulation by nucleosome positioning. *Trends in Genetics*. **26**, 476–483
12. Jenuwein, T., and Allis, C. D. (2001) Translating the Histone Code. *Science (1979)*. **293**, 1074–1080
13. Miller, M., Makaju, A., Wang, L., and Franklin, S. (2015) Histone Post-translational Modifications Differentially Regulated in a Mouse Mode of Heart Disease. *The FASEB Journal*. 10.1096/fasebj.29.1_supplement.570.15
14. Yang, Y., Luan, Y., Yuan, R.-X., and Luan, Y. (2021) Histone Methylation Related Therapeutic Challenge in Cardiovascular Diseases. *Front Cardiovasc Med*. 10.3389/fcvm.2021.710053
15. Cavalli, G., and Heard, E. (2019) Advances in epigenetics link genetics to the environment and disease. *Nature*. **571**, 489–499
16. Guiot, J., Struman, I., Chavez, V., Henket, M., Herzog, M., Scoubeau, K., Hardat, N., Bondue, B., Corhay, JL., Moermans, C., and Louis, R. (2017) Altered epigenetic features in circulating nucleosomes in idiopathic pulmonary fibrosis. *Clin Epigenetics*. **9**, 84
17. Baylin, S. B., and Jones, P. A. (2016) Epigenetic Determinants of Cancer. *Cold Spring Harb Perspect Biol*. **8**, a019505
18. Mancarella, D., and Plass, C. (2021) Epigenetic signatures in cancer: proper controls, current challenges and the potential for clinical translation. *Genome Med*. **13**, 23

19. Nebbioso, A., Tambaro, F. P., Dell'Aversana, C., and Altucci, L. (2018) Cancer epigenetics: Moving forward. *PLoS Genet*. **14**, e1007362
20. Pathak, A., Tomar, S., and Pathak, S. (2023) Epigenetics and Cancer: A Comprehensive Review. *Asian Pacific Journal of Cancer Biology*. **8**, 75–89
21. Audia, J. E., and Campbell, R. M. (2016) Histone Modifications and Cancer. *Cold Spring Harb Perspect Biol*. **8**, a019521
22. Zhao, Z., and Shilatifard, A. (2019) Epigenetic modifications of histones in cancer. *Genome Biol*. **20**, 245
23. García-Giménez, J. L., Seco-Cervera, M., Tollefsbol, T. O., Romá-Mateo, C., Peiró-Chova, L., Lapunzina, P., and Pallardó, F. V. (2017) Epigenetic biomarkers: Current strategies and future challenges for their use in the clinical laboratory. *Crit Rev Clin Lab Sci*. **54**, 529–550
24. Bauden, M., Pamart, D., Ansari, D., Herzog, M., Eccleston, M., Micallef, J., Andersson, B., and Andersson, R. (2015) Circulating nucleosomes as epigenetic biomarkers in pancreatic cancer. *Clin Epigenetics*. **7**, 106
25. Seligson, D. B., Horvath, S., Shi, T., Yu, H., Tze, S., Grunstein, M., and Kurdistani, S. K. (2005) Global histone modification patterns predict risk of prostate cancer recurrence. *Nature*. **435**, 1262–1266
26. Herceg, Z., and Hainaut, P. (2007) Genetic and epigenetic alterations as biomarkers for cancer detection, diagnosis and prognosis. *Mol Oncol*. **1**, 26–41
27. Yang, J., Xu, J., Wang, W., Zhang, B., Yu, X., and Shi, S. (2023) Epigenetic regulation in the tumor microenvironment: molecular mechanisms and therapeutic targets. *Signal Transduct Target Ther*. **8**, 210
28. Kelly, A. D., and Issa, J.-P. J. (2017) The promise of epigenetic therapy: reprogramming the cancer epigenome. *Curr Opin Genet Dev*. **42**, 68–77
29. Hassler, M. R., Schiefer, A.-I., and Egger, G. (2013) Combating the epigenome: epigenetic drugs against non-Hodgkin's lymphoma. *Epigenomics*. **5**, 397–415
30. Sahafnejad, Z., Ramazi, S., and Allahverdi, A. (2023) An Update of Epigenetic Drugs for the Treatment of Cancers and Brain Diseases: A Comprehensive Review. *Genes (Basel)*. **14**, 873
31. Zain, J., and O'Connor, O. A. (2010) Targeting histone deacetyalses in the treatment of B- and T-cell malignancies. *Invest New Drugs*. **28**, 58–78
32. Kawaf, R. R., Ramadan, W. S., and El-Awady, R. (2024) Deciphering the interplay of histone post-translational modifications in cancer: Co-targeting histone modulators for precision therapy. *Life Sci*. **346**, 122639
33. Sabi, S. H., Qnais, E. Y. A., Al Tall, Y. R., Almaaytah, A. M., and Masaadeh, M. M. (2023) Pharmaco-epigenetics: Histone modification and personalized medicine. *Pharmacia*. **70**, 337–349
34. Dejeux, E., Rønneberg, J. A., Solvang, H., Bukholm, I., Geisler, S., Aas, T., Gut, I. G., Børresen-Dale, A.-L., Lønning, P. E., Kristensen, V. N., and Tost, J. (2010) DNA methylation profiling in doxorubicin treated primary locally advanced breast tumours identifies novel genes associated with survival and treatment response. *Mol Cancer*. **9**, 68
35. Kronfol, M. M., Dozmorov, M. G., Huang, R., Slattum, P. W., and McClay, J. L. (2017) The role of epigenomics in personalized medicine. *Expert Rev Precis Med Drug Dev*. **2**, 33–45

36. Li, L., Choi, J.-Y., Lee, K.-M., Sung, H., Park, S. K., Oze, I., Pan, K.-F., You, W.-C., Chen, Y.-X., Fang, J.-Y., Matsuo, K., Kim, W. H., Yuasa, Y., and Kang, D. (2012) DNA Methylation in Peripheral Blood: A Potential Biomarker for Cancer Molecular Epidemiology. *J Epidemiol*. **22**, 384–394
37. Fridley, B. L., Armasu, S. M., Cicek, M. S., Larson, M. C., Wang, C., Winham, S. J., Kalli, K. R., Koestler, D. C., Rider, D. N., Shridhar, V., Olson, J. E., Cunningham, J. M., and Goode, E. L. (2014) Methylation of leukocyte DNA and ovarian cancer: relationships with disease status and outcome. *BMC Med Genomics*. **7**, 21
38. Koestler, D. C., Marsit, C. J., Christensen, B. C., Accomando, W., Langevin, S. M., Houseman, E. A., Nelson, H. H., Karagas, M. R., Wiencke, J. K., and Kelsey, K. T. (2012) Peripheral Blood Immune Cell Methylation Profiles Are Associated with Nonhematopoietic Cancers. *Cancer Epidemiology, Biomarkers & Prevention*. **21**, 1293–1302
39. Gavin, D. P., and Sharma, R. P. (2009) Chromatin from Peripheral Blood Mononuclear Cells as Biomarkers for Epigenetic Abnormalities in Schizophrenia. *Cardiovasc Psychiatry Neurol*. **2009**, 1–4
40. Manoel-Caetano, F. S., Xavier, D. J., Evangelista, A. F., Takahashi, P., Collares, C. V., Puthier, D., Foss-Freitas, M. C., Foss, M. C., Donadi, E. A., Passos, G. A., and Sakamoto-Hojo, E. T. (2012) Gene expression profiles displayed by peripheral blood mononuclear cells from patients with type 2 diabetes mellitus focusing on biological processes implicated on the pathogenesis of the disease. *Gene*. **511**, 151–160
41. Young, M. D., Willson, T. A., Wakefield, M. J., Trounson, E., Hilton, D. J., Blewitt, M. E., Oshlack, A., and Majewski, I. J. (2011) ChIP-seq analysis reveals distinct H3K27me3 profiles that correlate with transcriptional activity. *Nucleic Acids Res*. **39**, 7415–7427
42. Milne, T. A., Zhao, K., and Hess, J. L. (2009) Chromatin Immunoprecipitation (ChIP) for Analysis of Histone Modifications and Chromatin-Associated Proteins, pp. 409–423, 10.1007/978-1-59745-418-6_21
43. Vai, A., Noberini, R., Ghirardi, C., Rodrigues de Paula, D., Carminati, M., Pallavi, R., Araújo, N., Varga-Weisz, P., and Bonaldi, T. (2024) Improved Mass Spectrometry–Based Methods Reveal Abundant Propionylation and Tissue-Specific Histone Propionylation Profiles. *Molecular & Cellular Proteomics*. **23**, 100799
44. Noberini, R., Robusti, G., and Bonaldi, T. (2022) Mass spectrometry-based characterization of histones in clinical samples: applications, progress, and challenges. *FEBS J*. **289**, 1191–1213
45. Grolleau, E., Candiracci, J., Lescuyer, G., Barthelemy, D., Benzerdjeb, N., Haon, C., Geiguer, F., Raffin, M., Hardat, N., Balandier, J., Rabeuf, R., Chalabreysse, L., Wozny, A.-S., Rommelaere, G., Rodriguez-Lafrasse, C., Subtil, F., Couraud, S., Herzog, M., and Payen-Gay, L. (2023) Circulating H3K27 Methylated Nucleosome Plasma Concentration: Synergistic Information with Circulating Tumor DNA Molecular Profiling. *Biomolecules*. **13**, 1255
46. Van den Ackerveken, P., Lobbens, A., Turatsinze, J.-V., Solis-Mezarino, V., Völker-Albert, M., Imhof, A., and Herzog, M. (2021) A novel proteomics approach to epigenetic profiling of circulating nucleosomes. *Sci Rep*. **11**, 7256
47. Van den Ackerveken, P., Lobbens, A., Pamart, D., Kotronoulas, A., Rommelaere, G., Eccleston, M., and Herzog, M. (2023) Epigenetic profiles of elevated cell free circulating H3.1 nucleosomes as potential biomarkers for non-Hodgkin lymphoma. *Sci Rep*. **13**, 16335

48. Terrell, J., Josseaux, E., Latora, H., Rommelaere, G., Hardat, N., Herzog, M., Micallef, J., and Eccleston, M. (2020) Circulating nucleosomes in hematological malignancy. *Journal of Clinical Oncology*. **38**, e20078–e20078
49. Khan, S. A. (2015) Global histone post-translational modifications and cancer: Biomarkers for diagnosis, prognosis and treatment? *World J Biol Chem*. **6**, 333
50. Seligson, D. B., Horvath, S., McBrian, M. A., Mah, V., Yu, H., Tze, S., Wang, Q., Chia, D., Goodglick, L., and Kurdistani, S. K. (2009) Global Levels of Histone Modifications Predict Prognosis in Different Cancers. *Am J Pathol*. **174**, 1619–1628
51. Füllgrabe, J., Kavanagh, E., and Joseph, B. (2011) Histone onco-modifications. *Oncogene*. **30**, 3391–3403
52. Lin, Y., Qiu, T., Wei, G., Que, Y., Wang, W., Kong, Y., Xie, T., and Chen, X. (2022) Role of Histone Post-Translational Modifications in Inflammatory Diseases. *Front Immunol*. 10.3389/fimmu.2022.852272
53. Li, D., Zhang, L., He, Y., Zhou, T., Cheng, X., Huang, W., and Xu, Y. (2022) Novel histone post-translational modifications in diabetes and complications of diabetes: The underlying mechanisms and implications. *Biomedicine & Pharmacotherapy*. **156**, 113984
54. Araki, Y., and Mimura, T. (2017) The Histone Modification Code in the Pathogenesis of Autoimmune Diseases. *Mediators Inflamm*. **2017**, 1–12
55. Ramazi, S., Allahverdi, A., and Zahiri, J. (2020) Evaluation of post-translational modifications in histone proteins: A review on histone modification defects in developmental and neurological disorders. *J Biosci*. **45**, 135
56. Smith, B. J., and Carregari, V. C. (2022) Histone Modifications in Neurological Disorders, pp. 95–107, 10.1007/978-3-031-05460-0_7
57. El Kennani, S., Crespo, M., Govin, J., and Pflieger, D. (2018) Proteomic Analysis of Histone Variants and Their PTMs: Strategies and Pitfalls. *Proteomes*. **6**, 29
58. Gade, P., and Kalvakolanu, D. V. (2012) Chromatin Immunoprecipitation Assay as a Tool for Analyzing Transcription Factor Activity, pp. 85–104, 10.1007/978-1-61779-376-9_6
59. Li, Y. (2021) Modern epigenetics methods in biological research. *Methods*. **187**, 104–113
60. Tollefsbol, T. O. (2011) Advances in Epigenetic Technology, pp. 1–10, 10.1007/978-1-61779-316-5_1
61. Hattori, T., and Koide, S. (2018) Next-generation antibodies for post-translational modifications. *Curr Opin Struct Biol*. **51**, 141–148
62. Lu, C., Coradin, M., Porter, E. G., and Garcia, B. A. (2021) Accelerating the Field of Epigenetic Histone Modification Through Mass Spectrometry–Based Approaches. *Molecular & Cellular Proteomics*. **20**, 100006
63. Noberini, R., Restellini, C., Savoia, E. O., and Bonaldi, T. (2020) Enrichment of histones from patient samples for mass spectrometry-based analysis of post-translational modifications. *Methods*. **184**, 19–28
64. Mann, M., and Jensen, O. N. (2003) Proteomic analysis of post-translational modifications. *Nat Biotechnol*. **21**, 255–261
65. Van den Ackerveken, P., Lobbens, A., Turatsinze, J. V., Solis-Mezarino, V., Völker-Albert, M., Imhof, A., and Herzog, M. (2021) A novel proteomics approach to epigenetic profiling of circulating nucleosomes. *Sci Rep*. 10.1038/s41598-021-86630-3

66. Soldi, M., Cuomo, A., and Bonaldi, T. (2014) Improved bottom-up strategy to efficiently separate hypermodified histone peptides through ultra-HPLC separation on a bench top Orbitrap instrument. *Proteomics*. **14**, 2212–2225
67. Rodriguez-Collazo, P., Leuba, S. H., and Zlatanova, J. (2009) Robust methods for purification of histones from cultured mammalian cells with the preservation of their native modifications. *Nucleic Acids Res*. **37**, e81–e81
68. Shechter, D., Dormann, H. L., Allis, C. D., and Hake, S. B. (2007) Extraction, purification and analysis of histones. *Nat Protoc*. **2**, 1445–1457
69. Bonaldi, T., Imhof, A., and Regula, J. T. (2004) A combination of different mass spectroscopic techniques for the analysis of dynamic changes of histone modifications. *Proteomics*. **4**, 1382–1396
70. Ju, H., Lai, G., and Yan, F. (2017) Introduction. in *Immunosensing for Detection of Protein Biomarkers*, pp. 1–30, Elsevier, 10.1016/B978-0-08-101999-3.00001-3
71. Egelhofer, T. A., Minoda, A., Klugman, S., Lee, K., Kolasinska-Zwierz, P., Alekseyenko, A. A., Cheung, M.-S., Day, D. S., Gadel, S., Gorchakov, A. A., Gu, T., Kharchenko, P. V, Kuan, S., Latorre, I., Linder-Basso, D., Luu, Y., Ngo, Q., Perry, M., Rechtsteiner, A., Riddle, N. C., Schwartz, Y. B., Shanower, G. A., Vielle, A., Ahringer, J., Elgin, S. C. R., Kuroda, M. I., Pirrotta, V., Ren, B., Strome, S., Park, P. J., Karpen, G. H., Hawkins, R. D., and Lieb, J. D. (2011) An assessment of histone-modification antibody quality. *Nat Struct Mol Biol*. **18**, 91–93
72. Peach, S. E., Rudomin, E. L., Udeshi, N. D., Carr, S. A., and Jaffe, J. D. (2012) Quantitative Assessment of Chromatin Immunoprecipitation Grade Antibodies Directed against Histone Modifications Reveals Patterns of Co-occurring Marks on Histone Protein Molecules. *Molecular & Cellular Proteomics*. **11**, 128–137
73. Jeong, S., Park, M.-J., Song, W., and Kim, H.-S. (2020) Current immunoassay methods and their applications to clinically used biomarkers of breast cancer. *Clin Biochem*. **78**, 43–57
74. Cavalier, E., Guiot, J., Lechner, K., Dutsch, A., Eccleston, M., Herzog, M., Bygott, T., Schomburg, A., Kelly, T., and Holdenrieder, S. (2021) Circulating Nucleosomes as Potential Markers to Monitor COVID-19 Disease Progression. *Front Mol Biosci*. 10.3389/fmolb.2021.600881
75. Ananchuensook, P., Wongpiyabovorn, J., Avihingsanon, A., and Tangkijvanich, P. (2024) Performance of Elecsys® HCV Duo Immunoassay for Diagnosis and Assessment of Treatment Response in HCV Patients with or without HIV Infection. *Diagnostics*. **14**, 2179
76. Ueda, H., and Dong, J. (2023) Biosensors: Homogeneous Detection. in *Encyclopedia of Sensors and Biosensors*, pp. 458–477, Elsevier, 10.1016/B978-0-12-822548-6.00053-4
77. Slagle, K. M., and Ghosn, S. J. (1996) Immunoassays: Tools for Sensitive, Specific, and Accurate Test Results. *Lab Med*. **27**, 177–183
78. Das, P., and Taube, J. H. (2020) Regulating Methylation at H3K27: A Trick or Treat for Cancer Cell Plasticity. *Cancers (Basel)*. **12**, 2792
79. Ngollo, M., Lebert, A., Daures, M., Judes, G., Rifai, K., Dubois, L., Kemeny, J.-L., Penault-Llorca, F., Bignon, Y.-J., Guy, L., and Bernard-Gallon, D. (2017) Global analysis of H3K27me3 as an epigenetic marker in prostate cancer progression. *BMC Cancer*. **17**, 261

80. Hoffmann, F., Niebel, D., Aymans, P., Ferring-Schmitt, S., Dietrich, D., and Landsberg, J. (2020) H3K27me3 and EZH2 expression in melanoma: relevance for melanoma progression and response to immune checkpoint blockade. *Clin Epigenetics*. **12**, 24
81. He, J., Xu, T., Zhao, F., Guo, J., and Hu, Q. (2023) SETD2-H3K36ME3: an important bridge between the environment and tumors. *Front Genet*. 10.3389/fgene.2023.1204463
82. Elsheikh, S. E., Green, A. R., Rakha, E. A., Powe, D. G., Ahmed, R. A., Collins, H. M., Soria, D., Garibaldi, J. M., Paish, C. E., Ammar, A. A., Grainge, M. J., Ball, G. R., Abdelghany, M. K., Martinez-Pomares, L., Heery, D. M., and Ellis, I. O. (2009) Global Histone Modifications in Breast Cancer Correlate with Tumor Phenotypes, Prognostic Factors, and Patient Outcome. *Cancer Res*. **69**, 3802–3809
83. Liu, B., Cheng, J., Zhang, X., Wang, R., Zhang, W., Lin, H., Xiao, X., Cai, S., Chen, X., and Cheng, H. (2010) Global Histone Modification Patterns as Prognostic Markers to Classify Glioma Patients. *Cancer Epidemiology, Biomarkers & Prevention*. **19**, 2888–2896

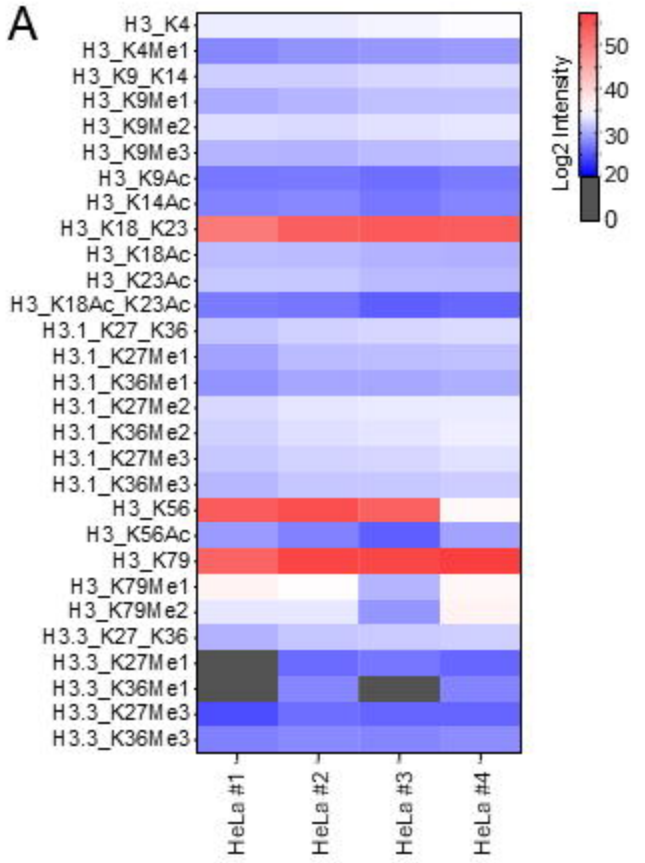
A
H3_K4
H3_K4Me1
H3_K9_K14
H3_K9Me1
H3_K9Me2
H3_K9Me3
H3_K9Ac
H3_K14Ac
H3_K18_K23
H3_K18Ac
H3_K23Ac
H3_K18Ac_K23Ac
H3.1_K27_K36
H3.1_K27Me1
H3.1_K36Me1
H3.1_K27Me2
H3.1_K36Me2
H3.1_K27Me3
H3.1_K36Me3
H3_K56
H3_K56Ac
H3_K79
H3_K79Me1
H3_K79Me2
H3.3_K27_K36
H3.3_K27Me1
H3.3_K36Me1
H3.3_K27Me3
H3.3_K36Me3
HeLa #1
HeLa #2
HeLa #3
HeLa #4
Log2 Intensity
50
40
30
20
0

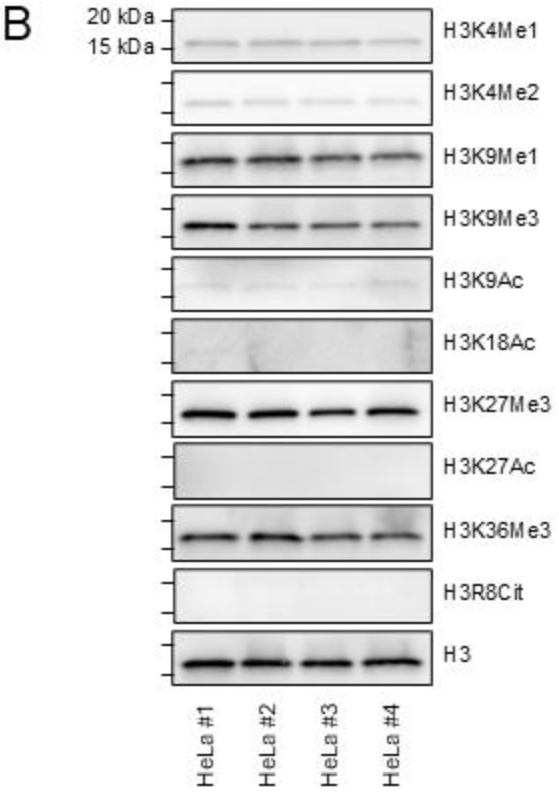
B
20 kDa
15 kDa
H3K4Me1
H3K4Me2
H3K9Me1
H3K9Me3
H3K9Ac
H3K18Ac
H3K27Me3
H3K27Ac
H3K36Me3
H3R8Cit
H3
HeLa #1
HeLa #2
HeLa #3
HeLa #4

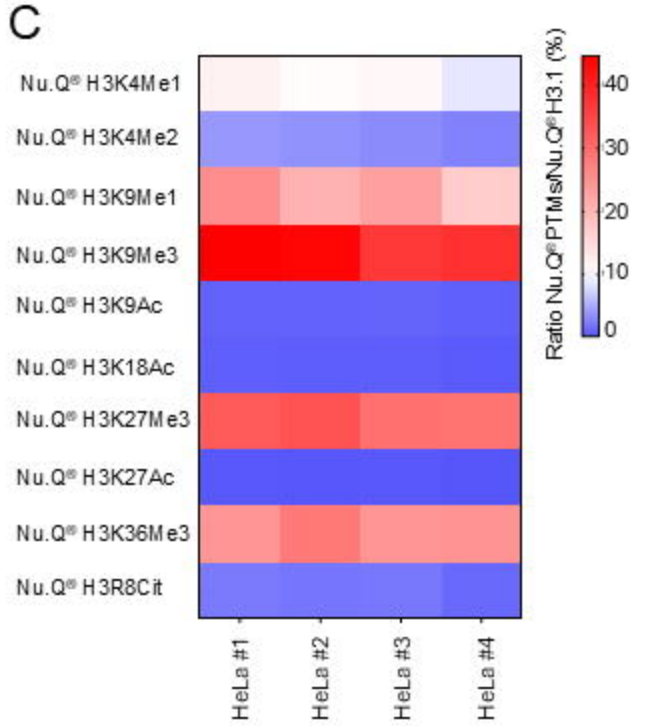
C
Nu.Q® H3K4Me1
Nu.Q® H3K4Me2
Nu.Q® H3K9Me1
Nu.Q® H3K9Me3
Nu.Q® H3K9Ac
Nu.Q® H3K18Ac
Nu.Q® H3K27Me3
Nu.Q® H3K27Ac
Nu.Q® H3K36Me3
Nu.Q® H3R8Cit
HeLa #1
HeLa #2
HeLa #3
HeLa #4
Ratio Nu.Q® PTMs/Nu.Q® H3.1 (%)
40
30
20
10
0

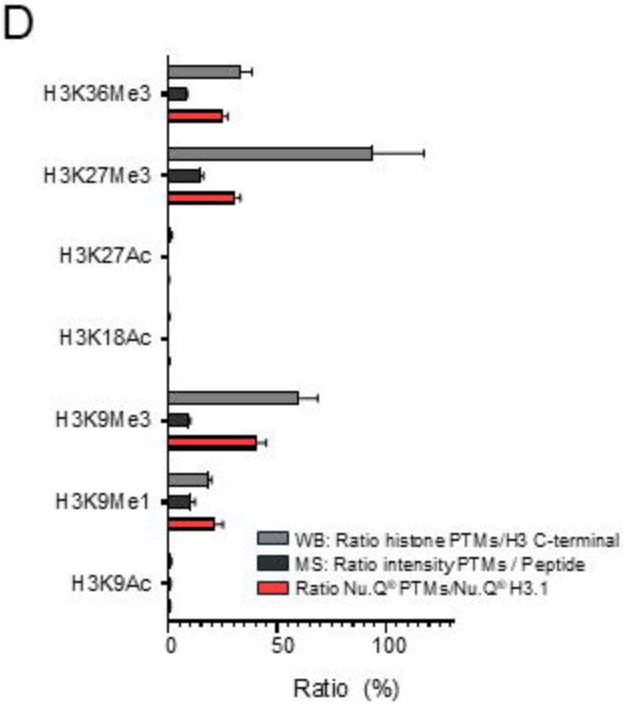
D
H3K36Me3
H3K27Me3
H3K27Ac
H3K18Ac
H3K9Me3
H3K9Me1
H3K9Ac
WB: Ratio histone PTMs/H3 C-terminal
MS: Ratio intensity PTMs / Peptide
Ratio Nu.Q® PTMs/Nu.Q® H3.1
0
50
100
Ratio (%)

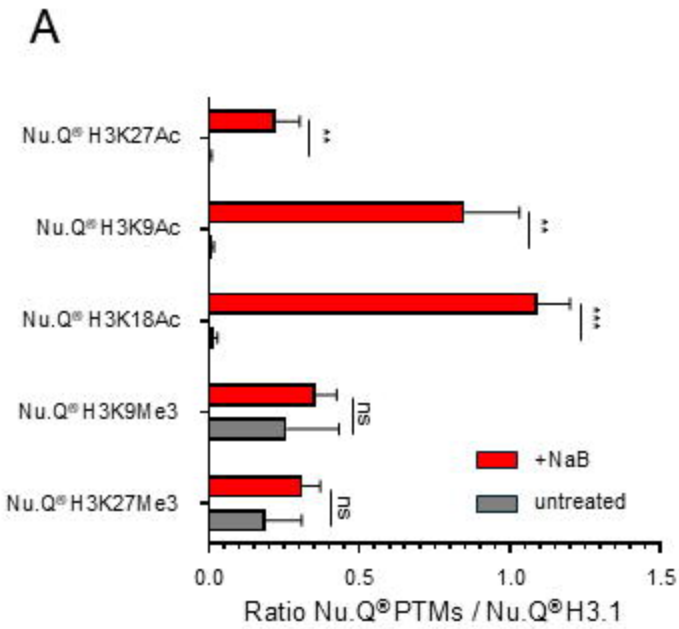
A
Nu.Q® H3K27Ac
Nu.Q® H3K9Ac
Nu.Q® H3K18Ac
Nu.Q® H3K9Me3
Nu.Q® H3K27Me3
**
**
***
ns
ns
+NaB
untreated
0.0
0.5
1.0
1.5
Ratio Nu.Q® PTMs / Nu.Q® H3.1

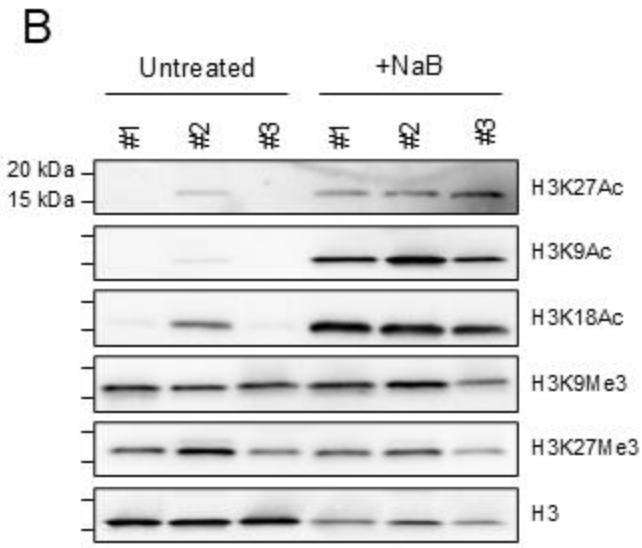
B
Untreated
+NaB
#1
#2
#3
#1
#2
#3
20 kDa
15 kDa
H3K27Ac
H3K9Ac
H3K18Ac
H3K9Me3
H3K27Me3
H3

A

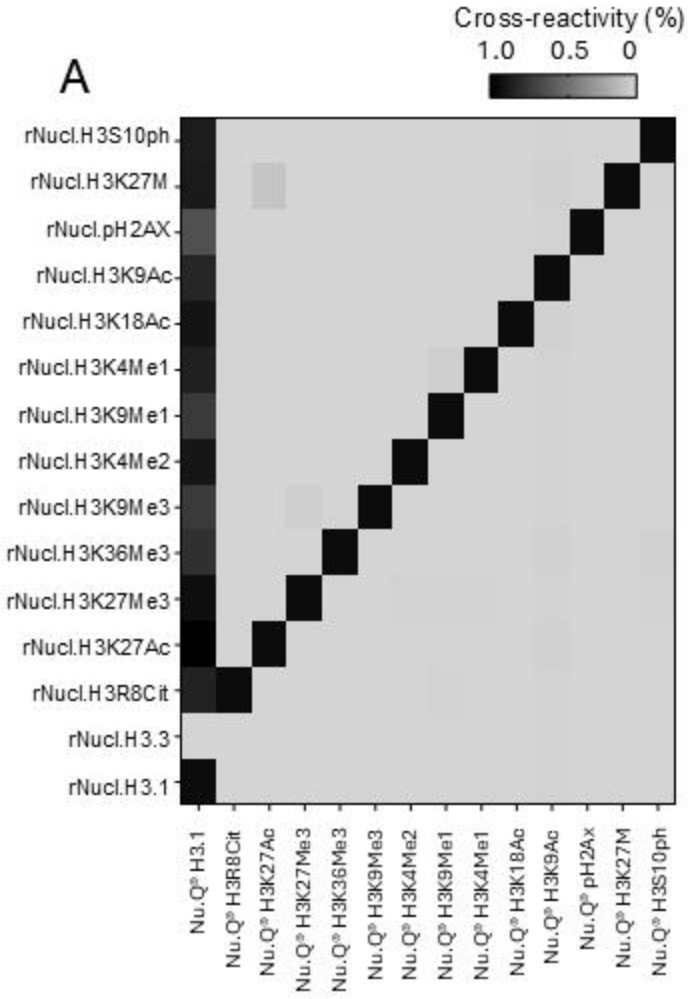

B

	Intra-CV (%)		Inter-CV (%)	
	Min.	Max.	Min.	Max.
Nu.Q® H3K27Me3	1.7	6.4	3.9	10.8
Nu.Q® H3R8Cit	2.4	3.0	4.4	16.1
Nu.Q® H3K27M	2.1	4.3	2.7	13.2
Nu.Q® H3K9Ac	2.6	7.6	3.9	11.4
Nu.Q® pH2AX	1.1	3.5	1.4	4.8
Nu.Q® H3S10ph	0.9	3.8	2.3	7.4
Nu.Q® H3K9Me1	1.5	2.6	3.2	7.3
Nu.Q® H3K36Me3	1.9	3.4	4.6	7.0
Nu.Q® H3K18Ac	1.1	1.7	5.8	8.3
Nu.Q® H3K27Ac	0.9	4.0	2.4	7.3
Nu.Q® H3K4Me2	1.3	2.2	3.8	5.1
Nu.Q® H3K4Me1	1.0	3.2	4.2	6.6
Nu.Q® H3K9Me3	1.4	3.6	2.5	9.1

C

ng/mL	LOB	LOD	LOQ
Nu.Q® H3K27Me3	0.48	2.24	2.79
Nu.Q® H3R8Cit	1.03	3.12	4.80
Nu.Q® H3K27M	1.90	3.27	2.08
Nu.Q® H3K9Ac	1.10	3.00	5.4
Nu.Q® pH2AX	0.60	0.80	0.80
Nu.Q® H3S10ph	0.20	0.90	1.70
Nu.Q® H3K9Me1	0.10	0.90	0.90
Nu.Q® H3K36Me3	1.14	2.11	8.10
Nu.Q® H3K18Ac	1.24	3.57	3.57
Nu.Q® H3K27Ac	0.24	1.00	1.00
Nu.Q® H3K4Me2	0.10	1.91	1.91
Nu.Q® H3K4Me1	0.24	0.88	1.98
Nu.Q® H3K9Me3	0.32	2.12	2.12

D

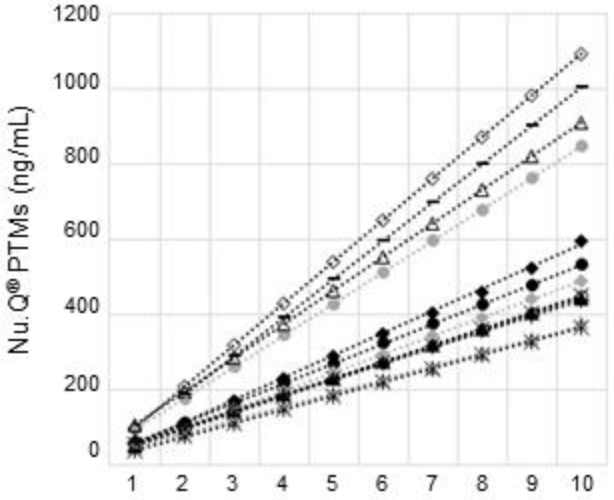

Assay	Linearity range (ng/mL)	R^2
Nu.Q® H3K27Me3	4.86 - 372.17	0.9993
Nu.Q® H3R8Cit	58.15 – 596.51	0.9985
Nu.Q® H3K27M	7.25 - 845.66	1.0000
Nu.Q® H3K9Ac	50.85 - 443.80	0.9997
Nu.Q® pH2AX	3.09 - 500.00	1.0000
Nu.Q® H3S10ph	17.99 - 489.80	1.0000
Nu.Q® H3K9Me1	6.52 - 444.59	1.0000
Nu.Q® H3K36Me3	5.66 - 911.18	1.0000
Nu.Q® H3K18Ac	27.40 - 1094.10	0.9994
Nu.Q® H3K27Ac	53.55 - 449.93	1.0000
Nu.Q® H3K4Me2	31.40 - 417.10	0.9999
Nu.Q® H3K4Me1	3.95 - 1005.95	1.0000
Nu.Q® H3K9Me3	60.67 - 439.40	1.0000

A

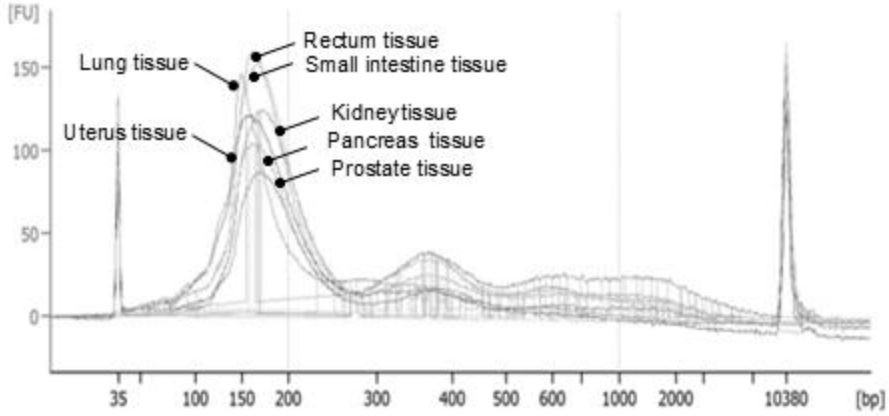
[FU]
150
100
50
0
Lung tissue
Uterus tissue
Rectum tissue
Small intestine tissue
Kidneytissue
Pancreas tissue
Prostate tissue
35
100
150
200
300
400
500
600
1000
2000
10380
[bp]

B

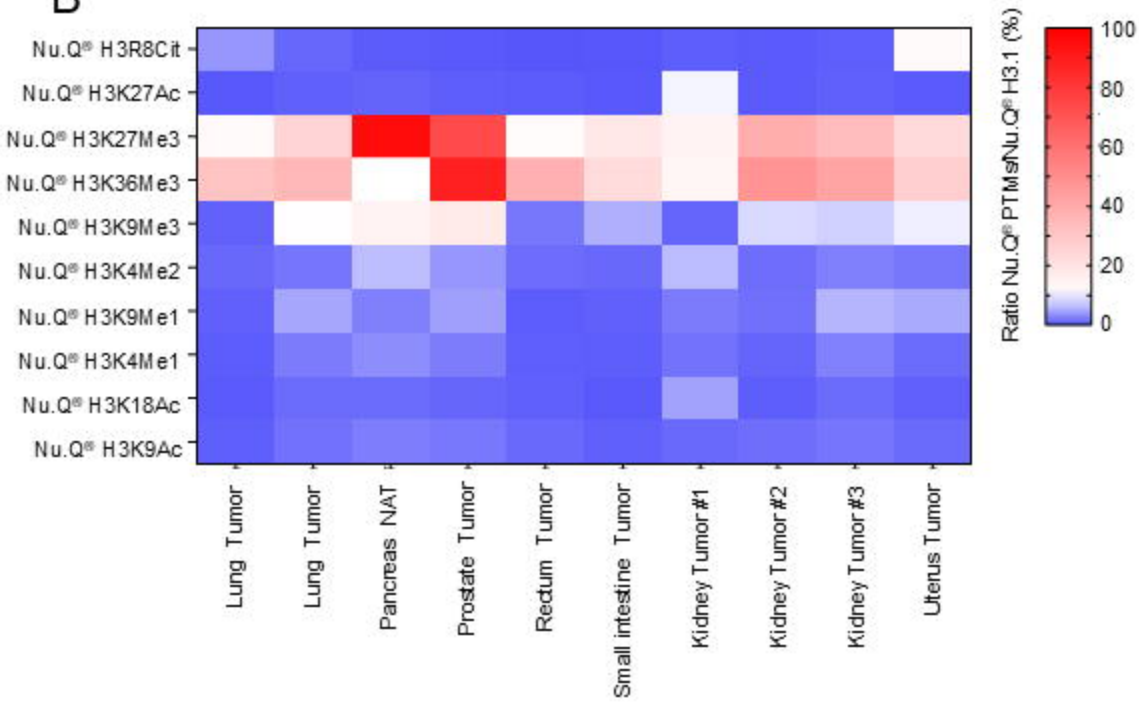
Nu.Q® H3R8Cit
Nu.Q® H3K27Ac
Nu.Q® H3K27Me3
Nu.Q® H3K36Me3
Nu.Q® H3K9Me3
Nu.Q® H3K4Me2
Nu.Q® H3K9Me1
Nu.Q® H3K4Me1
Nu.Q® H3K18Ac
Nu.Q® H3K9Ac
Lung Tumor
Lung Tumor
Pancreas NAT
Prostate Tumor
Rectum Tumor
Small intestine Tumor
Kidney Tumor #1
Kidney Tumor #2
Kidney Tumor #3
Uterus Tumor
Ratio Nu.Q® PTMs/Nu.Q® H3.1 (%)
100
80
60
40
20
0

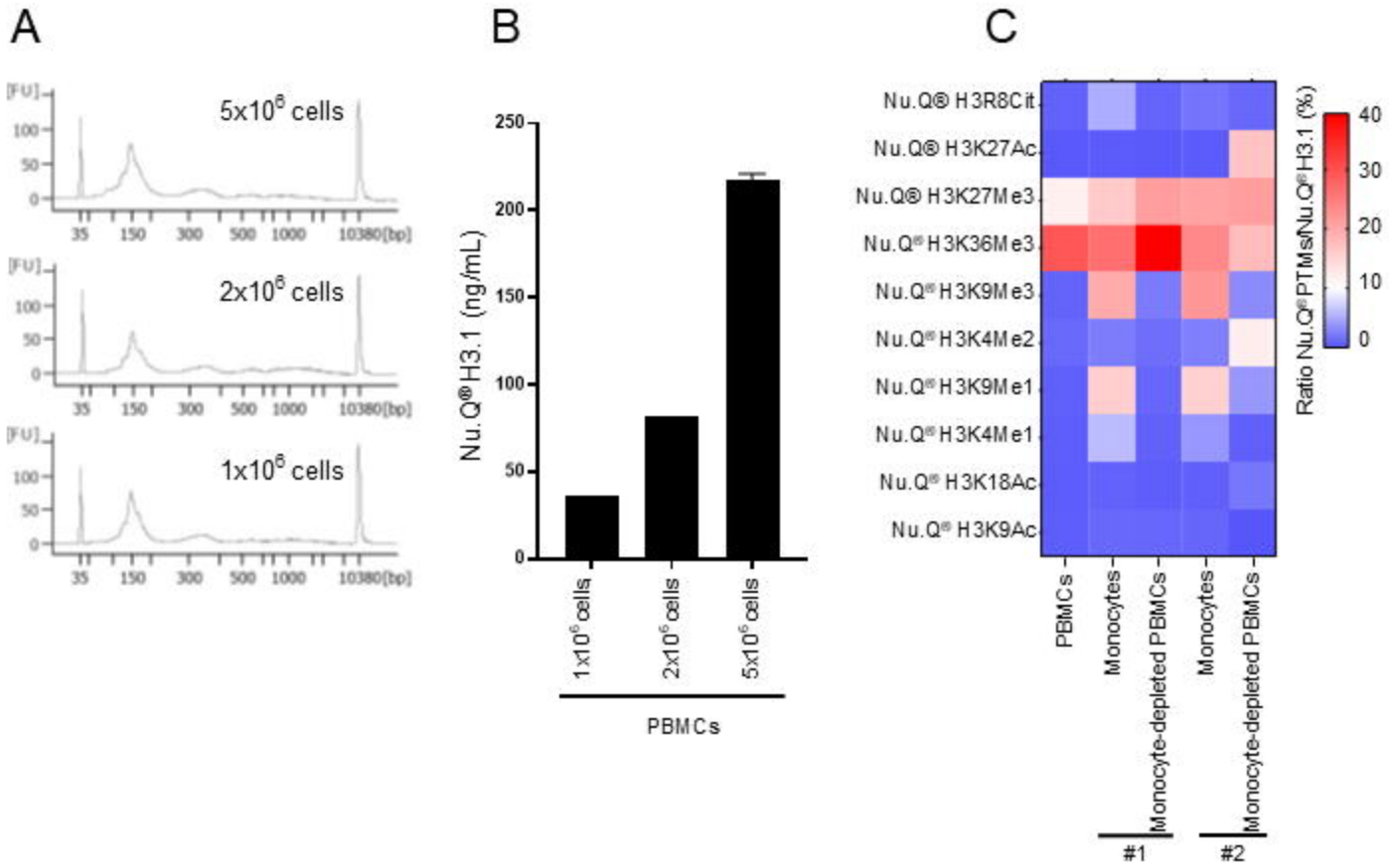
A
5x10^6 cells
2x10^6 cells
1x10^6 cells
[FU]
100
50
0
35
150
300
500
1000
10380[bp]
B
Nu.Q® H3.1 (ng/mL)
250
200
150
100
50
0
1x10^6 cells
2x10^6 cells
5x10^6 cells
PBMCs
C
Nu.Q® H3R8Cit
Nu.Q® H3K27Ac
Nu.Q® H3K27Me3
Nu.Q® H3K36Me3
Nu.Q® H3K9Me3
Nu.Q® H3K4Me2
Nu.Q® H3K9Me1
Nu.Q® H3K4Me1
Nu.Q® H3K18Ac
Nu.Q® H3K9Ac
PBMCs
Monocytes
Monocyte-depleted PBMCs
Monocytes
Monocyte-depleted PBMCs
#1
#2
Ratio Nu.Q® PTMs/Nu.Q® H3.1 (%)
40
30
20
10
0